Inorg. Chem. **2004**, *43*, 1902–1911

Cyanide-Melt Synthesis of Reduced Molybdenum Selenide Clusters

Carmela Magliocchi, Xiaobing Xie, and Timothy Hughbanks*

Department of Chemistry, Texas A&M University, P.O. Box 30012, College Station, Texas 77842-3012

Received September 5, 2003

The tightly cross-linked $Mo_{3n}Se_{3n+2}$ (n = 2, 3, ...∞) cluster compounds react with alkali metal cyanide or cyanide salt mixtures at temperatures of 450–675 °C to yield cyanide-terminated molybdenum chalcogenide clusters, $[Mo_6Se_8(CN)_6]^{n-}$ ($\mathbf{1}^{n-}$) (n = 6, 7) and $[Mo_4Se_4(CN)_{12}]^{8-}$ ($\mathbf{2}^{8-}$). The process by which discrete $\mathbf{1}^{n-}$ clusters are excised from a CN-linked intermediate chain compound, $K_6Mo_6Se_8(CN)_5$ (**3**), was investigated, and the cubane cluster $\mathbf{2}^{7-}$ plays an essential role. An efficient one-step synthesis for $Na_8[\mathbf{2}^{8-}]$ is presented. These clusters are stable in basic aqueous solutions. Cyclic voltammetric (CV) measurements in basic aqueous media show multiple reversible redox waves corresponding to $\mathbf{1}^{6-/7-}$, $\mathbf{1}^{7-/8-}$, and $\mathbf{1}^{8-/9-}$ redox couples with half-wave potentials of $E_{1/2}$ = –0.442, –0.876, and –1.369 V, respectively, versus SHE. Half-wave potentials ($E_{1/2}$) for the $[Mo_4Se_4(CN)_{12}]^{6-/7-}$ and $[Mo_4Se_4(CN)_{12}]^{7-/8-}$ couples are 0.233 and –0.422 V, respectively, versus SHE. The $\mathbf{2}^{8-}$ compounds are $K_7Na[\mathbf{2}^{8-}]\cdot 5H_2O\cdot MeOH$, $Cs_7Na_4[\mathbf{2}^{8-}]Cl_3$, $Na_8[\mathbf{2}^{8-}]$, and $K_4Na_4[\mathbf{2}^{8-}]\cdot 12H_2O$. The products were characterized by X-ray crystallography, cyclic voltammetry, and UV–vis spectroscopy. Reduction potentials measured by voltammetry are consistent with conditions needed for isolating reduced species on a preparative scale but are much more negative than previously reported values. $Na_8[\mathbf{1}^{8-}]\cdot 20H_2O$ was isolated by reduction of $\mathbf{1}^{7-}$ with Zn in aqueous NaCN solution. Reduction potentials measured in basic NaCN solutions of $\mathbf{2}^{8-}$ also differ widely from previous reported values.

Introduction

Thirty years ago, Sergent's group discovered the "Chevrel phases", $M_xMo_6Q_8$ (M = metal, Q = S, Se, Te). These compounds are of interest for their physical and chemical properties, such as high-critical-field (H_{c2}) superconductivity,[1] magnetic ordering,[2−5] fast ion conductivity,[6] and catalytic activity for hydrodesulfurization (HDS).[7] Fuller development of this chemistry revealed that Mo_6Q_8-cluster compounds are the first members of a series of compounds with the general composition $M_{n-2}Mo_{3n}Q_{3n+2}$ (M = alkali metal, Q = S, Se, Te, n = 2−10, 12, and ∞).[1,8−18] In compounds with finite n, oligomeric units exist in which the stacking of Mo_3Q_3 units is truncated by capping with a single chalcogenide atom at each end. The last of the members of the family (n = ∞) are the nanowire precursor compounds, $M^IMo_3Q_3$ (M^I = Na, K, Rb, Cs, Tl, In, Q = S, Se, Te), in which extended chains are built up of trans-face-sharing Mo_6Q_8 octahedra (or a stacking of staggered Mo_3Q_3 planar fragments). Clusters in all but the extended chain compounds are tightly cross-linked into three-dimensional extended frameworks by intercluster Mo−Q bonds.

Considerable recent effort has focused on isolation and derivatization of the molecular precursor $Mo_6Q_8L_6$ species in hopes that these electroactive clusters might be exploited in a variety of ways.[19,20] Until recently, preparation of Mo_6Q_8

* To whom correspondence should be addressed. E-mail: trh@mail.chem.tamu.edu.

(1) Chevrel, R.; Sergent, M. In *Topics in Current Physics, Vol. 32: Superconductivity in Ternary Compounds I: Structural, Electronic, and Lattice Properties*; Fischer, O., Maple, M. B., Eds.; Springer-Verlag: New York, 1982; Vol. 32, pp 25−83.
(2) Pena, O.; Sergent, M. *Prog. Solid State Chem.* **1989**, *19*, 165−281.
(3) Burlet, P.; Flouquet, J.; Genicon, J. L.; Horyn, R.; Pena, O.; Sergent, M. *Physica B (Amsterdam)* **1995**, *215*, 127−133.
(4) Pena, O.; LeBerre, F.; Sergent, M.; Horyn, R.; Wojakowski, A. *Physica C (Amsterdam)* **1994**, *235−240*, 771−772.
(5) Giroud, M.; Genicon, J. L.; Tournier, R.; Geantet, C.; Pena, O.; Horyn, R.; Sergent, M. *J. Low Temp. Phys.* **1987**, *69*, 419−450.
(6) Mulhern, P. J.; Haering, R. R. *Can. J. Phys.* **1984**, *62*, 527−531.
(7) McCarty, K. F.; Anderegg, J. W.; Schrader, G. L. *J. Catal.* **1985**, *93*, 375−387.
(8) Chevrel, R.; Sergent, M.; Prigent, J. *J. Solid State Chem.* **1971**, *3*, 515−519.
(9) Chevrel, R.; Gougeon, P.; Potel, M.; Sergent, M. *J. Solid State Chem.* **1985**, *57*, 25.
(10) Chevrel, R. In *Crystal Chemistry and Properties of Materials with Quasi-One-Dimensional Structures*; Rouxel, J., Ed.; Reidel: New York, 1986.
(11) Gougeon, P.; Potel, M.; Padiou, J.; Sergent, M. *Mater. Res. Bull.* **1987**, *22*, 1087−1093.
(12) Gougeon, P.; Potel, M.; Sergent, M. *Acta Crystallogr.* **1989**, *C45*, 182−185.
(13) Thomas, C.; Picard, S.; Gautier, R.; Gougeon, P.; Potel, M. *J. Alloys Compd.* **1997**, *262−263*, 305−310.
(14) Picard, S.; Potel, M.; Gougeon, P. *Angew. Chem., Int. Ed.* **1999**, *38*, 2034−2036.

10.1021/ic035050u CCC: $27.50
Published on Web 02/20/2004

clusters has involved either assembly from smaller clusters, such as $Mo_3Q_4Cl_4$ (Q = S, Se), or via capping-ligand exchange reactions beginning with the $[Mo_6Cl_8]^{4+}$ cluster core.[19,21] An alternative approach to cluster synthesis is the excision of clusters from thermodynamically stable solid-state cluster compounds. Holm and co-workers were able to excise Re_6Q_8 (Q = Se, Te) clusters from loosely cross-linked network compounds with the use of R_4NCl (R = Et, Pr, Bu) in hot DMF or MeCN.[22] Fedorov and co-workers reported that molten cyanides (NaCN or KCN) could be used to excise Re_6Q_8 clusters from extended structures, and they synthesized a series of new chalcogenide complexes containing the $[Re_6Q_8(CN)_6]^{4-}$ (Q = S, Se, Te) cluster complex.[23−26] Surprisingly, Fedorov's group was able to extend the use of cyanide melts to the more tightly cross-linked binary Chevrel phase compound Mo_6Se_8, obtaining discrete $[Mo_6Se_8(CN)_6]^{7-}$ (**1**$^{7-}$) and $[Mo_6Se_8(CN)_6]^{6-}$ (**1**$^{6-}$) cluster ions.[27]

In a previous communication, we reported that the reaction of molten KCN with Mo_6Se_8 or simpler starting materials (e.g., 2Mo + 4$MoSe_2$) yields a product, $K_6Mo_6Se_8(CN)_4(CN)_{2/2}$ (**3**), in which chains are built up from $Mo_6Se_8(CN)_4$ units that are bridged by cyanide ligands.[28] The use of simple starting materials demonstrated that molten KCN serves as a medium for the formation of Mo_6Se_8 clusters; there is no need to postulate a true "cluster excision" reaction even when a cluster compound is used as a starting material. Indeed, we show here that when reduced molybdenum chalcogenide compounds incorporating larger $[Mo_{12}Se_{14}]^{2-}$ clusters serve as starting materials, the larger clusters do not survive in the products. We report the synthesis and isolation of the reduced cluster compounds Cs_7Na_4[**2**$^{8-}$]Cl_3, K_7Na[**2**$^{8-}$]·$5H_2O$·MeOH, Na_8[**2**$^{8-}$], and K_4Na_4[**2**$^{8-}$]·$12H_2O$ and present results pertaining to the mechanism by which the chain compound **3** is dissolved. Also reported are systematic electrochemical measurements on the series of [**1**]$^{n-}$ and [**2**]$^{n-}$ clusters in aqueous solutions, and the preparation of a highly reduced cluster compound, Na_8[**1**$^{8-}$]·$20H_2O$.

Experimental Section

Techniques and Materials. All compounds were manipulated in a nitrogen atmosphere glovebox or on Schlenk (Ar) or high-vacuum lines. The solid-state precursors Mo_6Se_8, $Cs_2Mo_{12}Se_{14}$, $K_4Mo(CN)_8$·$2H_2O$, and K_7[**1**$^{7-}$]·$8H_2O$ were synthesized according to previously published procedures.[1,11,27,29] Molybdenum powder (99.999%, Alfa Aesar) was reduced under flowing H_2 atmosphere at 750 °C over 10 hours in order to eliminate traces of oxygen. CsCl (99.999%, Alfa Aesar), $AlCl_3$ (95%, Alfa Aesar) which was recrystallized, and 1-methyl,3-ethylimidazolium chloride (ImCl)[30] were dried under vacuum prior to use. $MoSe_2$ (99.9%, Alfa Aesar), KCN (98%, Sigma Aldrich), and NaCN (99.99%, Aldrich) powders were used as received. Preparations of the cluster precursors were verified by inspection of Guinier powder diffraction patterns and/or patterns measured on an X-ray powder diffractometer. Solutions and liquid reagents were manipulated with syringes and cannulas, which were first purged with argon or nitrogen. Deionized water was deoxygenated by bubbling with nitrogen gas for 1 day prior to storage in a nitrogen-purged box.

$Na_8[Mo_6Se_8(CN)_6]$·$20H_2O$ (4). K_7[**1**$^{7-}$]·$8H_2O$ was prepared by reaction of Mo_6Se_8 with molten KCN, following the method of Fedorov and co-workers.[27] In a 15 mL ampule, $K_7[Mo_6Se_8(CN)_6]$·$8H_2O$ (0.1 g, 0.0562 mmol) was dissolved in 10 mL of deoxygenated water to form an intense dark blue solution. The solution was added to a 50 mL flask with NaCN (0.4 g, 8.1621 mmol) and Zn powder (0.4 g, 6.1171 mmol) and stirred for 10 min whereupon the original color first changed to violet and then darkened to maroon. After letting this solution stand for several hours, it was separated from unreacted zinc by filtration and transferred into another 100 mL flask containing 30 mL of distilled methanol, whereupon a dark red precipitate formed. The solvent was removed by a second filtration and then dried under vacuum. When dried, the precipitate had a red-purplish color and weighed 0.077 g (67% yield). Suitable crystals for X-ray diffraction measurements were grown in-situ from the reduced solution still in contact with Zn powder that was layered with distilled methanol and sealed on a Schlenk line. After 3 days, deeply colored crystals were observed on the walls of the tube below a colorless supernatant. Crystals were mounted in Paratone, in which they retained a deep red color consistent with **1**$^{8-}$; crystals mounted in silicone grease or Apiezon changed color, indicating oxidation to form **1**$^{7-}$.

$K_7Na[Mo_4Se_4(CN)_{12}]$·$5H_2O$·MeOH (5). Before a method of obtaining **2**$^{8-}$ in good yield had been devised (see **8**, below), a much less efficient method had been used to obtain cubane clusters. Since we have made use of products from those syntheses in this paper, this method is described briefly here. In two separate trials, Finely ground Mo and $MoSe_2$ were combined in a 1:3 (first trial) or 1:1 (second trial) ratios with 20 equiv of NaCN and loaded into a fused silica tube and sealed under a dynamic vacuum. After heating at 500 °C for 60 h, the reaction mixture was cooled and then washed with deoxygenated H_2O for 30 min. Upon dissolution, burgundy solutions and undissolved solids were noted. The mixtures were filtered, and the burgundy filtrates containing the excess NaCN were separated from unreacted Mo and $MoSe_2$ and as-yet-uncharacterized black solids. To the resulting burgundy solutions, methanol was added until the supernatants became colorless and red solids had precipitated. The solids were dried under vacuum for 1 day; 0.051 g (trial 1) and 0.045 g (trial 2) portions of

(15) Gautier, R.; Picard, S.; Gougeon, P.; Potel, M. *Mater. Res. Bull.* **1999**, *34*, 93−101.
(16) Gougeon, P.; Potel, M.; Sergent, M. *Acta Crystallogr.* **1990**, *C46*, 2284−2287.
(17) Picard, S.; Gougeon, P.; Potel, M. *Acta Crystallogr.* **2001**, *C57*, 663−664.
(18) Picard, S.; Gougeon, P.; Potel, M. *Acta Crystallogr.* **2001**, *C57*, 335−336.
(19) Hilsenbeck, S. J.; Young, V. G., Jr.; McCarley, R. E. *Inorg. Chem.* **1994**, *33*, 1822−1832.
(20) Hilsenbeck, S. J.; McCarley, R. E.; Goldman, A. I. *Chem. Mater.* **1995**, *7*, 499−506.
(21) McCarley, R. E.; Hilsenbeck, S. J.; Xie, X. *J. Solid State Chem.* **1995**, *117*, 269−274.
(22) Yaghi, O. M.; Scott, M. J.; Holm, R. H. *Inorg. Chem.* **1992**, *31*, 4778−4784.
(23) Mironov, Y. V.; Cody, J. A.; Albrecht-Schmitt, T. E.; Ibers, J. A. *J. Am. Chem. Soc.* **1997**, *119*, 493−498.
(24) Naumov, N. G.; Virovets, A. V.; Podberezskaya, N. V.; Fedorov, V. E. *J. Struct. Chem.* **1998**, *38*, 857−862.
(25) Naumov, N. G.; Virovets, A. V.; Sokolov, M. N.; Artemkina, S. B.; Fedorov, V. E. *Angew. Chem., Int. Ed.* **1998**, *37*, 1943−1945.
(26) Mironov, Y. V.; Fedorov, V. E.; McLauchlan, C. C.; Ibers, J. A. *Inorg. Chem.* **2000**, *39*, 1809−1811.
(27) Mironov, Y. V.; Virovets, A. V.; Naumev, N. G.; Ikorskii, V. N.; Fedorov, V. E. *Chem. Eur. J.* **2000**, *6*, 1361−1365.
(28) Magliocchi, C.; Xie, X.; Hughbanks, T. *Inorg. Chem.* **2000**, *39*, 5000−5001.
(29) Leipoldt, J. G.; Bok, L. D. C.; Cilliers, P. J. *Z. Anorg. Allg. Chem.* **1974**, *407*, 350−352.
(30) Hussey, C. L. In *Chemistry of Nonaqueous Solutions*; Mamantov, G., Popov, A. I., Eds.; VCH: New York, 1994; pp 227−276.

$Na_7K[2^{8-}]\cdot 5H_2O\cdot MeOH$ were collected (~5% yield). Addition of more deoxygenated water to the remaining black solid residues extracted no further product. To obtain crystals, the filtrate was transferred into a tube and then layered with methanol and sealed under vacuum. Red rodlike crystals of $K_7Na[2^{8-}]\cdot 20H_2O$ were obtained after 1 week.

$Na_4Cs_7[Mo_4Se_4(CN)_{12}]Cl_3$ (6). Finely ground $Cs_2Mo_{12}Se_{14}$ (0.100 g, 0.0396 mmol), NaCN (0.388 g, 0.792 mmol), and CsCl (0.267 g, 1.585 mmol) were combined and loaded into a fused silica tube that was evacuated and sealed under dynamic vacuum. The tube was heated to 500 °C over 12 h, then maintained at that temperature for 24 h. The tube was cycled twice between temperatures of 450 and 500 °C for 24 h at each temperature and steadily cooled over 30 h to room temperature. Red crystals of $Na_4Cs_7[\mathbf{2}^{8-}]Cl_3$ appropriate for X-ray structure determination were obtained by heating of the reaction mixture in a substantial temperature gradient (425−500 °C) and gathering crystals that had formed at the cooler end of the reaction tube.

$Na_8[Mo_4Se_4(CN)_{12}]$ (7) and $Na_4K_4[Mo_4Se_4(CN)_{12}]\cdot 12H_2O$ (8). $K_4Mo(CN)_8\cdot 2H_2O$ was prepared following the method outlined by Leipoldt, and its identity was confirmed with powder XRD.[29] $K_4Mo(CN)_8\cdot 2H_2O$ was heated to 170 °C under vacuum, and the remaining $K_4Mo(CN)_8$ was used directly; thermal gravimetric analysis was used to verify quantitative loss of water. Finely ground $K_4Mo(CN)_8$ (0.193 g, 0.4180 mmol), Mo (0.041 g, 0.4180 mmol), $MoSe_2$ (0.212 g, 0.8360 mmol), and NaCN (0.164 g, 2.5178 mmol) were combined and loaded into a fused silica tube that was evacuated and sealed under vacuum. The tube was heated to 500 °C over 24 h, maintained at this temperature for 60 h, and cooled to room temperature over 24 h. The tube was opened, and the product was dissolved in 50 mL of deoxygenated water to give a deep burgundy solution that was filtered from undissolved black solid (determined to be unreacted Mo and $MoSe_2$ by powder XRD). To the burgundy solution was added 150 mL of distilled methanol, whereupon a reddish brown precipitate formed. The contents of the flask were once again filtered, and the solid product was dried under vacuum (0.281 g; 56% yield). To obtain crystals, the filtrate was transferred into a tube and then layered with methanol and sealed under vacuum. Red platelike crystals of $Na_8[\mathbf{2}^{8-}]\cdot 20H_2O$ were obtained after 3 weeks.

To obtain crystals directly, another reaction tube was loaded and heated in exactly the same manner, then cycled twice between temperatures of 450 and 500 °C for 24 h at each temperature, and steadily cooled over 30 h to room temperature. Red crystals of $Na_8[\mathbf{2}^{8-}]$ (**7**) appropriate for X-ray structure determination were obtained by heating of the reaction mixture in a substantial temperature gradient (425−500 °C) and gathering crystals that had formed at the cooler end of the reaction tube.

X-ray Structure Determinations. Single crystal structure determinations were undertaken for five cluster compounds (**4**−**8**). In every case but **4**, a crystal was coated with Apiezon-T grease immediately upon removal from its mother solution, then was mounted on the tip of a glass fiber or loop, and inserted into the low-temperature nitrogen stream of the diffractometer for data collection. Data were collected using a Siemens (Bruker) SMART CCD (charge coupled device) equipped diffractometer with a LT-2 low-temperature apparatus.

The first 50 frames were re-collected at the end of data collection to check for decay. Cell parameters were retrieved using SMART software[31] and refined using SAINT software[32] on all observed reflections. Data reduction was performed using SAINT, which corrects for Lorentz polarization and decay. For **4**, **7**, and **8**, the SADABS[33] absorption correction was applied. For **5** and **6**, multiscan absorption corrections were applied.

Initial molybdenum and selenium positions were obtained from SHELXL-97 direct methods output. The other non-hydrogen atomic positions were located from the electron density difference maps. Full-matrix least-squares structural refinements were performed on F^2 using the SHELXL-97 package,[34] incorporated in the SHELXTL-PC, v5.10 program.[35] Except as described, anisotropic displacement parameters were refined for all non-hydrogen atoms. No hydrogen atoms were included in final structure refinements. For **6**, disorder was found among the chloride ions. Charge balance requirements led us to expect three chloride ions per formula unit. One chlorine atom, Cl(1), resides on the 3-fold axis and refined uneventfully at full occupancy. Electron density peaks were found at three additional positions, Cl(21), Cl(22), and Cl(23), all in the same vicinity in the structure. A Cl atom was placed on each site and assigned an isotropic displacement parameter of 0.03 (equal to that for Cl(1)), and the occupancies were refined. At this point, the sum of these occupancies was such that we obtained 1.99 additional Cl atoms. We therefore completed the refinement by allowing displacement of the these atoms to vary, subject to the restraint that the combined population of Cl(21), Cl(22), and Cl(23) sites yielded 2.00(1) Cl atoms.

In **8**, similar disorder was found among two of the oxygen atoms, O(61) and O(62), for which electron density for O(6) was split between O(61) and O(62), which were separated by 0.91 Å. These two positions refined to ~1.00 additional O atom. Once again, we allowed the displacement of the these atoms to vary, subject to the restraint that the combined population of O(61) and O(62) sites yielded 1.00(1) O atoms. Positions for the five remaining oxygen atoms, O(1)−O(5), refined at full occupancy. Packing of the $[Mo_4Se_4(CN)_{12}]^{8-}$ clusters is pseudotetragonal (as in $P\bar{4}2_1m$), and this is reflected in the similarity of the *a* and *b* axis lengths (11.744(2) and 11.849(2) Å). A twin was present (~13%) as well, generated by a 2-fold rotation about the [110] axis, and this was accounted for by use of the TWIN in the SHELXTL program during the refinement. Despite the presence of the twin, anisotropic displacements could be refined for all atoms but C(1), C(3), and C(3), which gave at least one nonpositive displacement parameter. Pertinent crystallographic data for all compounds are summarized in Table 1.

Electrochemical Studies. To study $\mathbf{1}^{n-}$ species, 10 mg of $K_7[\mathbf{1}^{7-}]\cdot 8H_2O$ was reduced according to the procedure described above to make 7 mL of an $[\mathbf{1}^{8-}]$ solution (~0.3 M NaCN). For study of $\mathbf{2}^{n-}$ species, 10 mg of $K_7Na[\mathbf{2}^{8-}]\cdot 5H_2O\cdot MeOH$ (**5**) was added to 7 mL of deoxygenated water with 100 mg of NaCN (~0.3 M NaCN). Each solution was transferred into a customized 5-mL five-neck flask, on which each neck was covered by a septum; three of the necks are used to pass through electrodes, and when necessary, two necks allow for purging with inert gas. CV experiments were carried out with a BAS 100B/W electrochemical workstation (Bioanalytical Systems, West Lafayette, IN). A glassy carbon disk electrode served as a working electrode, the counter electrode was platinum wire, and the reference electrode was AgCl/Ag in 3 M aqueous NaCl solution. The potentials are reported versus

(31) *SMART*, V 4.043 ed.; Bruker Analytical X-ray System: Madison, WI, 1995.
(32) *SAINTPLUS* ,V 4.035 ed.; Madison, WI, 1999.
(33) Sheldrick, G. M. Institute für Anorganishe Chemie der Universität Göttingen: Göttingen, Germany, 1999.
(34) Sheldrick, G. M. Institute für Anorganishe Chemie der Universität Göttingen: Göttingen, Germany, 1997.
(35) *SHELXTL* 5.10 (PC-version) ed.; Bruker Analytical X-ray Systems: Madison, WI, 1998.

Table 1. Crystallographic Data for Reduced Molybdenum Cluster Compounds

	4 $Na_8[Mo_6Se_8(CN)_6]\cdot 20H_2O$	**5** $NaK_7[Mo_4Se_4(CN)_{12}]\cdot 5H_2O\cdot MeOH$	**6** $Na_4Cs_7[Mo_4Se_4(CN)_{12}]Cl_3$	**7** $Na_8[Mo_4Se_4(CN)_{12}]$	**8** $K_4Na_4[Mo_4Se_4(CN)_{12}]\cdot 12H_2O$
fw, g/mol	1867.36	1420.57	2273.43	1195.76	1452.20
space group	$P\bar{1}$	$P2_12_12_1$	$R3m$	$I4_1/amd$	$P2_12_12$
a, Å	10.5887(14)	11.8498(5)	11.5386(10)	15.362(2)	11.744(2)
b, Å	10.7696(14)	12.2360(6)	11.5836(10)	15.362(2)	11.849(2)
c, Å	11.6714(15)	24.4645(11)	28.264(3)	11.055(2)	14.331(3)
α, deg	105.587(3)	90	90	90	90
β, deg	111.282(2)	90	90	90	90
γ, deg	104.176(2)	90	120	90	90
V, Å^3	1104.2(2)	3547.2(3)	3258.8(6)	2609.0(7)	1994.3(7)
Z	1	4	3	4	2
T (K)	110(2)	110(2)	110(2)	110(2)	110(2)
λ (Mo Kα) (Å)	0.71073	0.71073	0.71073	0.71073	0.71073
ρ_{calcd}, g/cm^3	2.808	2.660	3.475	3.044	2.418
μ (mm^{-1})	8.390	6.370	11.337	7.626	5.402
R1[a] ($I > 2\sigma(I)$)	0.0436	0.0203	0.0448	0.0462	0.0357
wR2[b]	0.1006	0.0492	0.0794	0.1013	0.0951

[a] $R1 = \sum||F_o| - |F_c||/\sum|F_o|$. [b] $wR2 = [\sum[w(|F_o|^2 - |F_c|^2)^2]/\sum[w(|F_o|^2)^2]]^{0.5}$.

Scheme 1

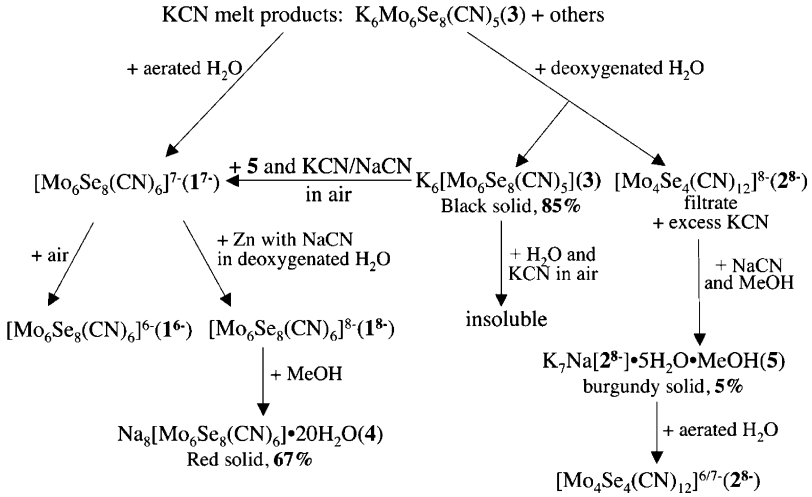

standard hydrogen electrode (SHE) and therefore are shifted by +0.222 V from the values measured.

Other Physical Measurements. Routine X-ray powder diffraction data were collected using Cu Kα ($\lambda = 1.5406$ Å) radiation on a Philips X-ray generator with a mounted Guinier camera or using the GADDS (general area detector diffraction system) V4.1.08 by Bruker AXS. UV−vis absorption spectra were measured with a Hewlett-Packard spectrophotometer. ^{13}C NMR spectra were recorded on Varian XL 300 broadband spectrometer (75.432 MHz for ^{13}C).

Results and Discussion

Synthesis of Reduced Molybdenum Chalcogenide Compounds. Scheme 1 summarizes the chemistry surrounding the synthesis of molybdenum selenide clusters in KCN melts, the dissolution of solid products, and isolation of discrete cluster products. Unless otherwise indicated, anionic species are in aqueous solution. The use of several alternative Mo- and Se-containing starting materials demonstrates that clusters need not be synthesized, but spontaneously form in the cyanide melts.[28]

As noted by Fedorov and co-workers,[27] products in the cooled cyanide melt can be directly dissolved in aerated water to obtain a $[Mo_6Se_8(CN)_6]^{6-/7-}$ ($\mathbf{1}^{6-/7-}$) mixture. In an earlier communication, we noted that there were undetermined species in the filtrate that are subject to oxidation upon exposure to air. Once obtained as a pure solid, the CN-bridged $K_6[Mo_6Se_8(CN)_5]$ (**3**, the principal product of these reactions) resists dissolution in strongly basic solutions or concentrated cyanide solutions. It follows that the "undetermined species" are essential to dissolution of **3**. It is now clear that the undetermined species are the cubane clusters, $[Mo_4Se_4(CN)_{12}]^{n-}$ ($\mathbf{2}^{n-}$, Figure 1).

In aerated aqueous solution, $\mathbf{1}^{7-}$ is slowly oxidized to yield $\mathbf{1}^{6-}$, but this does not occur in deoxygenated water. With rigorous exclusion of oxygen, red solutions of $\mathbf{1}^{8-}$ can be obtained by reduction over excess Zn powder. This reduced form is isolated as $Na_8[\mathbf{1}^{8-}]\cdot 20H_2O$ (**4**) upon addition of methanol, but $\mathbf{1}^{8-}$ efficiently scavenges oxygen and solutions stored in the absence of the Zn reductant often have a red-violet color, indicating contamination by $\mathbf{1}^{7-}$. The structure of $\mathbf{1}^{8-}$ is shown in Figure 2.

Role of $[Mo_4Se_4(CN)_{12}]^{7-}$ in Dissolution of $K_6Mo_6Se_8(CN)_5$. Clues to the dissolution of **3** became apparent when $\mathbf{2}^{8-}$ was obtained as a side product from reactions intended to produce the reduced $[Mo_6Se_8(CN)_6]^{8-}$

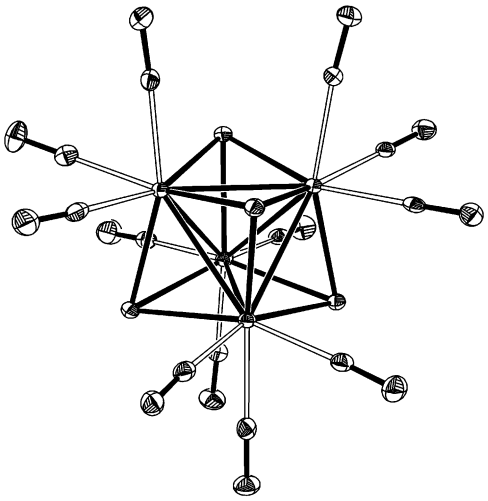

Figure 1. Cluster anion $[Mo_4Se_4(CN)_{12}]^{n-}$ in **5**. Ellipsoids are shown at 50% probability level.

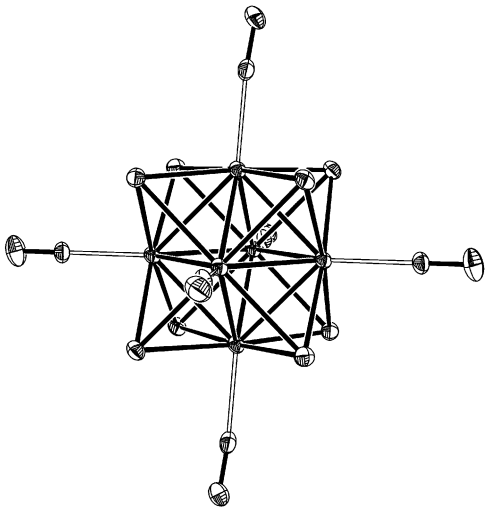

Figure 2. The $[Mo_6Se_8(CN)_6]^{8-}$ cluster in **4**. Ellipsoids are shown at 70% probability level.

cluster. After using the Fedorov protocol to prepare $K_7[Mo_6Se_8(CN)_6]\cdot 8H_2O$,[27] aqueous solutions were prepared for the purpose of reducing $\mathbf{1}^{7-}$. Compound $\mathbf{1}^{8-}$ was obtained in a reaction with zinc, but $\mathbf{2}^{8-}$ also crystallized as the hydrated salt $Na_8[Mo_4Se_4(CN)_{12}]\cdot 22H_2O$ upon workup. In further experimentation, pure $\mathbf{2}^{8-}$ cubane cluster compounds, $Na_7K[\mathbf{2}^{8-}]\cdot 5H_2O\cdot$MeOH (**5**) and $Na_4Cs_7[\mathbf{2}^{8-}]Cl_3$ (**6**), were isolated in low but reproducible yields. The 8− charge on the cluster complex ($\mathbf{2}^{8-}$) in **6** is definitively established since there are no potentially deprotonated solvent molecules that would make the total charge on the counterions ambiguous. Compound **6** was obtained in an attempt to excise clusters with the $Mo_{12}Se_{14}$ core from the precursor solid $Cs_2Mo_{12}Se_{14}$; we think it is likely that $\mathbf{2}^{8-}$ is present as a minor side product in most, if not all, of our reactions aimed at making $\mathbf{1}^{7-}$ in cyanide melts.

A number of methods exist for the preparation of the Mo/Se/CN cubane clusters. These methods are generally time-consuming and give low yields.[36−38] In our own experiments with the reduced cubane clusters, $\mathbf{2}^{8-}$, methods employing simple starting materials, Mo and $MoSe_2$, in synthesizing **5** also gave low yields (∼5% net yield), with a only slight improvement when the Chevrel phase, Mo_6Se_8 (17% yield) was used in its place. Because the cubane clusters play an important role in this chemistry, we sought a simple and efficient method for their synthesis. The efficient synthesis of **7** makes use of an additional reagent, $K_4Mo(CN)_8$, to achieve balance both with respect to the Mo/Se ratio but also with respect to the molybdenum oxidation state:

$$8NaCN + K_4Mo(CN)_8 + Mo + 2MoSe_2 \rightarrow Na_8[Mo_4Se_4(CN)_{12}] + 4KCN$$

Our observations indicate that air oxidation of $\mathbf{2}^{8-}$ must occur before dissolution of the chain compound **3** (to yield $\mathbf{1}^{6/7-}$) can occur. Compound $\mathbf{2}^{8-}$ is extracted as a soluble product that can be isolated without detectable oxidation when the product of a cyanide-melt reaction is washed thoroughly with deoxygenated water. If $\mathbf{2}^{8-}$ is separated from **3** in this way, **3** is insoluble even in oxygenated aqueous KCN solution. However, if air oxidation occurs to generate $\mathbf{2}^{7-}$, dissolution proceeds readily. If a solution of $\mathbf{2}^{7-}$ is added to the solid **3** under anaerobic conditions, **3** begins to dissolve, but the process stops after a short period of time. Electrochemical measurements (see below) show that the potential for the $\mathbf{2}^{7/8-}$ couple ($E_{1/2} = -0.422$ V) is quite close to that for the $\mathbf{1}^{6/7-}$ couple ($E_{1/2} = -0.442$ V). We propose that the sequence of events depicted in Scheme 2 transpires: $\mathbf{2}^{7-}$ promotes the dissolution of the chain compound **3** in a reaction wherein the Mo_6Se_8 core is oxidized and the $\mathbf{1}^{6-}$ cluster is the initially generated product that becomes involved in a redox equilibrium reaction with $\mathbf{2}^{8-}$: $\mathbf{1}^{6-} + \mathbf{2}^{8-} = \mathbf{1}^{7-} + \mathbf{2}^{7-}$. When oxygen is excluded, the concentration of $\mathbf{2}^{7-}$ is suppressed as the concentration of $\mathbf{1}^{7-}$ grows. The use of an excess of the stronger oxidant $[Fe(CN)_6]^{3-}$ promotes dissolution of the solid **3** (but if air is excluded, **3** remains insoluble), and at a much slower rate if no free cyanide is added. In solutions containing $\mathbf{2}^{7-}$, **3** dissolves overnight, whereas with $[Fe(CN)_6]^{3-}$ the process takes several weeks. If free cyanide is added, $[Fe(CN)_6]^{3-}$ promotes dissolution at a rate similar to that observed with $\mathbf{2}^{7-}$. This suggests that labile cyano ligands bound to $\mathbf{2}^{7-}$ may become involved in the reaction breaking the bridged links in **3**, and the greater effectiveness of $\mathbf{2}^{7-}$ (vs $[Fe(CN)_6]^{3-}$) in dissolving **3** stems from the greater lability of cyano ligands on the cubane complex.

Structures. $Na_8Mo_6Se_8(CN)_6\cdot 20H_2O$ (**4**) crystallizes in the triclinic space group $P\bar{1}$, with one molecule per unit cell. An ORTEP rendering of $\mathbf{1}^{8-}$ is shown in Figure 2. The cluster anion $\mathbf{1}^{8-}$ has an octahedral core of six molybdenum atoms with eight face-capping selenium atoms and terminal cyanide ligands coordinated to molybdenum atoms through the carbon atom. The Na^+ ions and the O positions were omitted

(36) Hernandez-Molina, R.; Sykes, A. G. *J. Chem. Soc., Dalton Trans.* **1999**, 3137−3148.

(37) Virovets, A. V.; Fedin, V. P.; Samsonenko, D. G.; Clegg, W. *Acta Crystallogr.* **2000**, *C56*, 272−273.

(38) Fedin, V. P.; Samsonenko, D. G.; Virovets, A. V.; Kalinina, I. V.; Naumov, D. Y. *Russ. Chem. Bull.* **2000**, *49*, 19−25.

Scheme 2

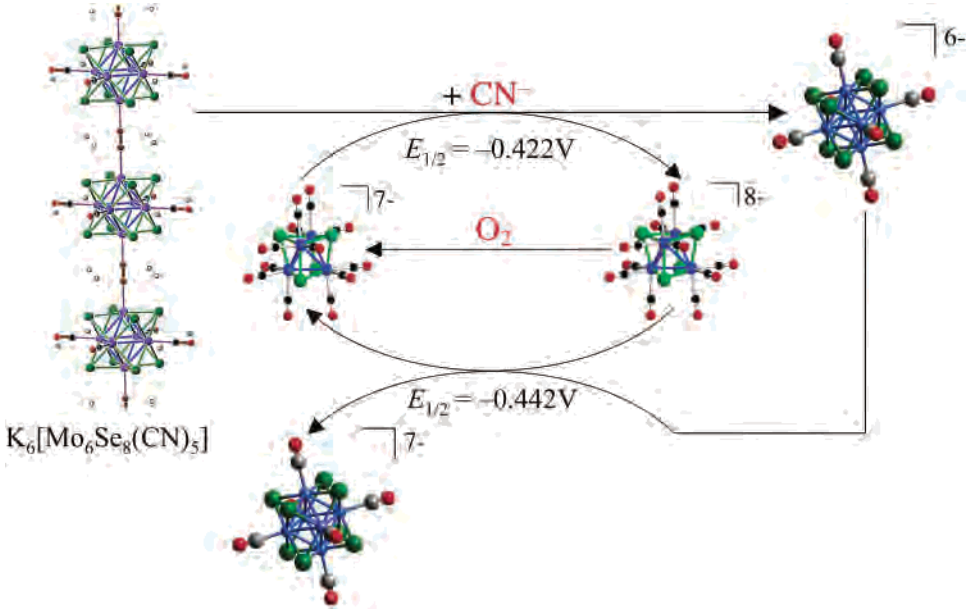

Table 2. Some Geometrical Characteristics of Mo_6Se_8 Cluster Cores (Distances (Å) and Angles (deg))

	$Na_8[Mo_6Se_8(CN)_6]\cdot 20H_2O$ (**5**)	$K_6Mo_6Se_8(CN)_5$ (**3**)[28]	$K_7[Mo_6Se_8(CN)_6]\cdot 8H_2O$[27]	$(Me_4N)_4K_2[Mo_6Se_8(CN)_6]\cdot 10H_2O$[27]	Mo_6Se_8[1]
Mo_6Se_8 *V*, Å^3	1104.2(2)	1260.5(1)	3761.5(8)	1448.5	797
d(Mo−Mo) range	2.6752(9)−2.7599(10)	2.6711(4)−2.7193(4)	2.700(3)	2.700(2)−2.721(2)	2.684(2)−2.836(2)
d(Mo−Mo) av	2.710	2.703	2.700	2.711	2.761
d(Mo−Se) range	2.559(1)−2.636(1)	2.5683(3)−2.5873(3)			2.547(2)−2.587(2)
d(Mo−Se) av	2.588	2.5763			2.568
d(Mo−C)	2.182(8)	2.204(3)			
d(C≡N)	1.169(9)	1.159(6)			
∠Mo−C−N	174.9(7)	180.0(1)			

for clarity. Geometric characteristics of the $\mathbf{1}^{8-}$ core are presented in Table 2. The Mo_6 octahedron exhibits a distortion of approximately tetragonal symmetry. A listing of the Mo−Mo bond distances (Å) clearly splits into two ranges, {2.6614(10), 2.6752(9), 2.6877(10), 2.6985(9)} and {2.7511(9), 2.7599(9)}; the six other distances are related by inversion symmetry. As we shall discuss below, four long bonds all lie in one basal plane of the octahedron, suggesting the occurrence of a pseudo-Jahn−Teller distortion; the Mo atoms are labeled according to whether they are in this large basal plane (Mo_b) or are sitting on an apical position (Mo_a). There is a less marked, but still noticeable, difference in the Mo−Se bond distances involving apical or basal Mo atoms: all Mo_b−Se distances are less than 2.60 Å (2.559(1)−2.595(1) Å), and all Mo_a−Se distances are greater than 2.60 Å (2.607(1)−2.636(1) Å). These distances are in the general ranges observed in many related Mo_6Se_8 compounds.[1,27,28] Comparison of the average Mo−Mo bond lengths for the 20-electron $\mathbf{1}^{6-}$ (2.711(5) Å), the 21-electron $\mathbf{1}^{7-}$ (2.700(3) Å), and the 22-electron $\mathbf{1}^{8-}$ (2.710(5) Å) reveals little concerning the bonding character of the orbital(s) populated upon reduction, consistent modest changes seen by other workers for molecular $Mo_6Se_8L_6$ clusters. For example, on moving from $[Mo_6Se_8(PEt_3)_6]$ to $[Mo_6Se_8(PEt_3)_6]^-$, the Mo−Mo bond lengthens by 0.010(1) Å.[39] In W_6Te_8 analogues, the opposite change is seen: on moving from $[W_6Te_8(py)_6]$ to $[W_6Te_8(py)_6]^-$ the W−W bond shortens by 0.010(1) Å.[40]

This reduced complex formally has 22 electrons involved in the metal−metal bonding with a HOMO electron configuration of e_g^2 and $^3A_{2g}$ triplet ground state in the O_h symmetry. If the anion is truly a triplet, this configuration should not give rise to a distortion in the octahedral core and is most likely due to the packing of eight Na^+ ions around the cluster anion in the crystal. ^{13}C NMR studies did not show any peaks (due to broadening), consistent with the existence of unpaired electrons. If the system is closed shell and octahedral, one sharp peak would be visible.

The structure of the cluster anion in **5** is shown in Figure 1, and the clusters in **6**, **7**, and **8** are virtually identical. $K_7Na[\mathbf{2}^{8-}]\cdot 5H_2O\cdot MeOH$ (**5**) crystallizes in the orthorhombic space group $P2_12_12_1$ with four clusters in the unit cell. $Na_4Cs_7[\mathbf{2}^{8-}]Cl_3$ (**6**) crystallizes in the rhombohedral space group *R*3*m* with 1 (3) cluster(s) per rhombohedral (hexagonal) unit cell. Both **6** and $Na_8[\mathbf{2}^{8-}]$ (**7**) contain no protic solvent molecules that might make the cluster oxidation state ambiguous. The molybdenum and chalcogen atoms form fairly regular cubane-type cores, and every molybdenum

(39) Saito, T.; Yamamoto, N.; Nagase, T.; Tsuboi, T.; Kobayashi, K.; Yamagata, T.; Imoto, H.; Unoura, K. *Inorg. Chem.* **1990**, *29*, 764−770.
(40) Xie, X.; McCarley, R. E. *Inorg. Chem.* **1997**, *36*, 4665−4675.

Table 3. Some Geometrical Characteristics of Mo_4Se_4 Cluster Cores (Distances (Å) and Angles (deg))

	$K_7Na[Mo_4Se_4(CN)_{12}]\cdot 5H_2O\cdot MeOH$ (**5**)	$Na_4Cs_7[Mo_4Se_4(CN)_{12}]Cl_3$ (**6**)	$(NH_4)_6[Mo_4Se_4(CN)_{12}]\cdot 6H_2O$[37]	$[Mo_4Se_4(H_2O)_{12}]\text{-}[pts]_5\cdot 14H_2O$[50]
Mo_4Se_4 *V*, Å^3	3547.2(3)	3258.8(6)	1806.9(3)	2023.98
d(Mo−Mo) range	2.901(1)−2.925(1)	2.910(1)−2.913(1)		2.791(4)−2.918(4)
d(Mo−Mo) av	2.910	2.912	2.886	2.865
d(Mo−Se) range	2.4927(5)−2.5219(5)	2.506(1)−2.510(1)		2.462(4)−2.485(4)
d(Mo−Se) av	2.506	2.507	2.502	2.479
d(Mo−C)	2.174(4)	2.158(16)	2.17(2)	
d(C≡N)	1.159(5)	1.179(2)	1.13(2)	
∠C−Mo−C	81(1)	79.3(1)	82.6	

atom is coordinated by three CN^- ligands. The $[Mo_4Se_4]$ cores exhibit only slight departures from ideal T_d point symmetry; all Mo−Mo and Mo−Se distances in **5** are within 0.01 Å of their mean values (2.910 and 2.507 Å, respectively), and those in the C_{3v}-symmetry clusters in **6** are within 0.001 Å of their averages (2.911 and 2.507 Å, respectively). Similar remarks apply to **7**; the average Mo−Mo and Mo−Se distances are 2.900 and 2.500 Å. These cubane clusters are isostructural with the Mo/S, Mo/Te W/S, W/Se, and W/Te analogues.[38,41] Some geometrical characteristics are presented in Table 1. Although crystal structures of $[Mo_4Se_4(H_2O)_{12}]^{5+}$ and $[Mo_4Se_4(CN)_{12}]^{6-}$ have been reported, $[Mo_4Se_4(CN)_{12}]^{8-}$ is the most reduced Mo_4Se_4-based species that has been structurally characterized to date.[37,50] The Mo−Mo bond distances are only slightly longer than reported for $\mathbf{2}^{6-}$ (2.886(4) Å) in $(NH_4)_6[Mo_4Se_4(CN)_{12}]\cdot 6H_2O$,[37] suggesting that the HOMO for $\mathbf{2}^{8-}$ is virtually Mo−Mo nonbonding (Table 3).

Electrochemical Properties. Electronic Structure and Bonding. Interpretation of the electrochemical behavior of $\mathbf{1}^{n-}$ and $\mathbf{2}^{n-}$ species is enhanced by an understanding of clusters' electronic structure. Theoretical treatments of $[Mo_6Q_8L_6]$ clusters indicate that Mo−Mo bonding is maximized when the number of cluster bonding electrons (CBEs) is 24, i.e., when 12 Mo−Mo bonding orbitals are occupied.[42] The Mo−Mo bonding molecular orbitals have a_{1g}, t_{1u}, t_{2g}, t_{2u}, and e_g symmetry, the last of which is variably occupied in clusters with 20−24 CBEs. The $[Mo_6Se_8]^0$ core has only 20 CBEs, and hence has a $a_{1g}^2t_{1u}^6t_{2g}^6t_{2u}^6e_g^0$ configuration. One or more electrons occupy the e_g LUMO in clusters with anionic Mo_6Se_8 cores. The reduced $\mathbf{1}^{8-}$ complex discussed above has 22 electrons and an e_g^2 configuration. In the O_h symmetry, we would expect a $^3A_{2g}$ ground state. However, we observed an appreciable "tetragonal" distortion (see above) in the solid state structure of $Na_8[\mathbf{2}^{8-}]\cdot 20H_2O$ that may favor a singlet ground state. We did not observe any resonances for the cyanide ligands in ^{13}C NMR spectra for $\mathbf{2}^{8-}$ suggesting that the ion may be paramagnetic in solution.

Elementary bonding considerations and more extensive calculations[38,43−45] indicate that $\mathbf{2}^{n-}$ clusters can accommodate up to 12 CBEs in 6 Mo−Mo bonding orbitals (of a_1, e, and t_2 symmetry for the T_d cluster). We have performed density functional theory (DFT-BLYP) calculations for $Na_4Cs_7[\mathbf{2}^{8-}]Cl_3$ using a single *k*-point ($k = 0$) in a band structure calculation; the local point symmetry of the $\mathbf{2}^{8-}$ ion was virtually C_{3v}, though not rigorously so, because an ordering of the disordered Cl^- ions had to be imposed. It should be noted that this treatment imbeds the $\mathbf{2}^{8-}$ ion in a realistic solid state Madelung potential, in contrast with several recently published calculations on metal cluster polyanions in vacuo.[46] More details of the calculation are available in the Supporting Information.

In the $\mathbf{2}^{n-}$ cluster core, each Mo atom is involved in 3 kinds of bonds: Mo−Mo, Mo−C(N), and Mo−Se. Each Mo atom is six-coordinate if we restrict our attention to the selenide and cyanide ligands. This distorted "octahedral" ligand environment leaves three "t_{2g}-like" d orbitals per Mo atom available for Mo−Mo bond formation. With four Mo atoms per cluster, we therefore expect to find 12 frontier MOs that are predominantly 4d in character and which are ordered in energy according to whether they are Mo−Mo bonding or antibonding. Figure 3 shows the frontier orbitals from both a DFT ($k = 0$) calculation on solid $Na_4Cs_7[\mathbf{2}^{8-}]Cl_3$ and an extended Hückel calculation for the $\mathbf{2}^{8-}$ ion. The latter results make clearer the T_d symmetry orbital correlations that can be made with the C_{3v} symmetry labeling that must be applied to the DFT results. These correlations ($T_d \rightarrow C_{3v}$: $a_1 \rightarrow a_1$, $a_2 \rightarrow a_2$, $e \rightarrow e$, $t_1 \rightarrow e + a_2$, $t_2 \rightarrow e + a_1$) show that the effects of lower C_{3v} symmetry environment on the cluster bonding are slight, as expected. There are six Mo−Mo bonding orbitals, of a_1, e, and t_2 symmetry (T_d labels), and six Mo−Mo antibonding orbitals (t_2 and t_1). Note that, in the calculation for $Na_4Cs_7[\mathbf{2}^{8-}]Cl_3$, the lowest lying Mo−Mo bonding orbital is sandwiched between orbitals with Cl^- 3p character. The most striking difference between the DFT and EH results is in the HOMO−LUMO gap; notably, the orbital gaps computed with DFT more closely correspond to the observed absorption bands (Figure 4), a maximum at 450 nm (2.75 eV) and a shoulder at 520 nm (2.38 eV). Magnetic measurements for $Na_4K_4[\mathbf{2}^{8-}]\cdot 12H_2O$ are fully consistent with the electronic description given above. Magnetic measurements for $Na_4K_4[\mathbf{2}^{8-}]\cdot 12H_2O$ are consistent with the expected diamagnetism of $\mathbf{2}^{8-}$, though a small portion of the sample is likely oxidized since a "Curie-tail"

(41) Fedin, V. P.; Kalinina, I. V.; Samsonenko, D. G.; Mironov, Y. V.; Sokolov, M. N.; Thackev, S. V.; Virovets, A. V.; Podberezskaya, N. V. *Inorg. Chem.* **1999**, *38*, 1956−1965.
(42) Hughbanks, T.; Hoffmann, R. *J. Am. Chem. Soc.* **1983**, *105*, 1150−1162.
(43) Mueller, A.; Jostes, R.; Eltzner, W.; Nie, C.; Diemann, E.; Boegge, H.; Zimmermann, M.; Dartmann, M.; Reinsch-Vogell, U. *Inorg. Chem.* **1985**, *24*, 2872−2884.
(44) Lu, S.; Huang, J.; Zhuang, H.; Li, J.; Wu, D.; Huang, Z.; Lu, C.; Huang, J.; Lu, J. *Polyhedron* **1991**, *10*, 2203−2215.
(45) Harris, S. *Polyhedron* **1989**, *8*, 2843−2882.
(46) Gray, T. G.; Rudzinski, C. M.; Meyer, E. E.; Holm, R. H.; Nocera, D. G. *J. Am. Chem. Soc.* **2003**, *125*, 4755−4770.

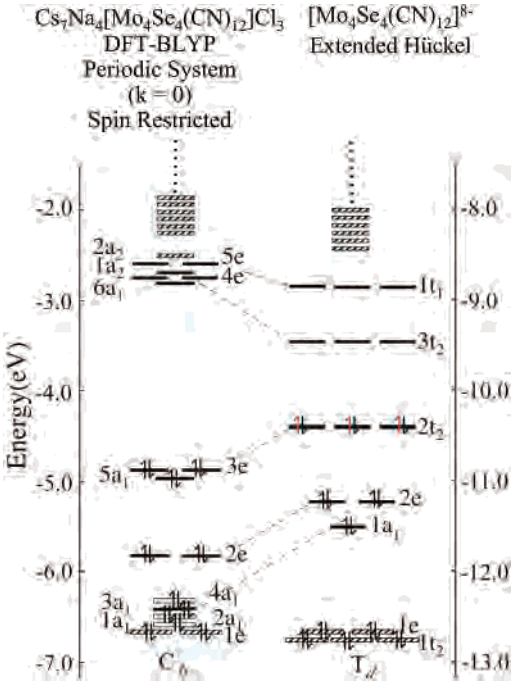

Figure 3. DFT-BLYP energy level diagram for solid $Na_4Cs_7[Mo_4Se_4(CN)_{12}]Cl_3$ (**6**) compared with extended Hückel calculated MO energy level diagram of $[Mo_4Se_4(CN)_{12}]^{8-}$ cluster ion. The black lines represent the Mo−Mo bonding and antibonding orbitals. The striped lines represent the orbitals with Se lone-pair character, and the hollow lines represent Cl^- localized orbitals.

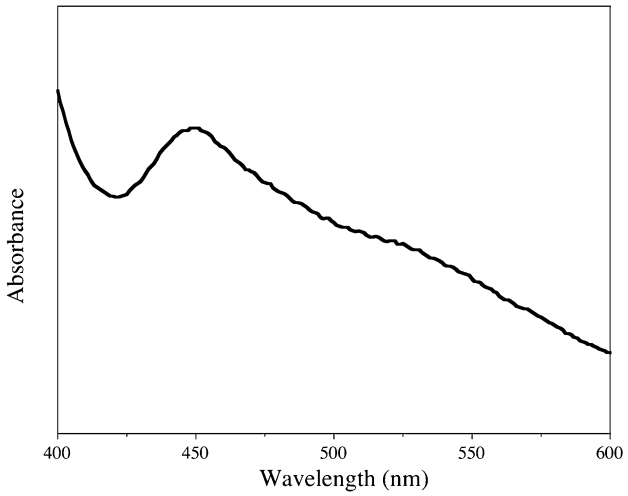

Figure 4. UV−vis absorption spectrum of **5** (1 mM solution).

characteristic of a paramagnetic impurity is observed at low temperatures.

Cyclic Voltammetry. A cyclic voltammogram recorded for a deep blue solution prepared by dissolving $K_7[\mathbf{1}^{7-}]\cdot 8H_2O$ in aqueous KCN is shown in Figure 5a. Upon scanning the potential in the negative direction from 0.222 V (0.0 V vs Ag/AgCl), three distinct redox waves are observed at $E_{1/2} = -0.442$, -0.876, and -1.369 V. When measurements were performed using the reduced cluster $Na_8[\mathbf{1}^{8-}]\cdot 20H_2O$ in 0.3 M aqueous NaCN, the voltammogram was virtually identical and the rest potential was −0.894 V. We attribute these redox waves to $\mathbf{1}^{6-/7-}$, $\mathbf{1}^{7-/8-}$, and $\mathbf{1}^{8-/9-}$ redox couples, respectively. Careful treatment of the electrode is necessary to observe the $\mathbf{1}^{8-/9-}$ couple, and the "reversibility" of these processes

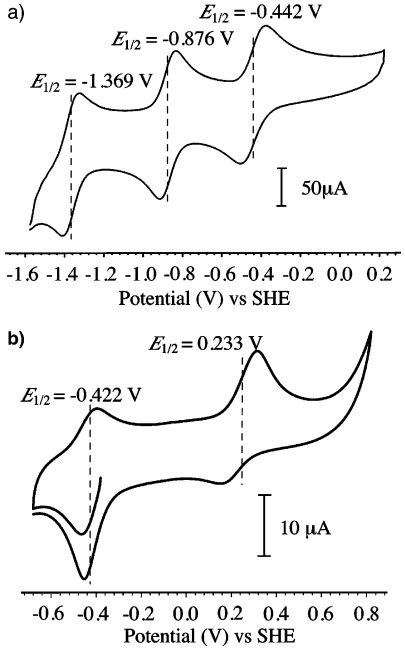

Figure 5. Cyclic voltammograms for aqueous solutions: (a) $K_7[Mo_6Se_8(CN)_6]\cdot 8H_2O$ (1 mM) in 0.25 M KOH or KCN, 500 mV/s scan rate. (b) $Na_8[Mo_4Se_4(CN)_{12}]\cdot 5H_2O\cdot MeOH$ (1.2 mM) in 0.3 M NaCN, 100 mV/s scan rate.

Table 4. Summary of Voltammetric Data for $[Mo_6Se_8(CN)_6]^{n-}$ and $[Mo_4Se_4(CN)_{12}]^{n-}$ Clusters in Basic Aqueous Solutions (Potentials vs SHE)

redox couple	$E_{1/2}$, V	ΔE_p, V	i_p^c/i_p^a
$[Mo_6Se_8(CN)_6]^{6-/7-}$	−0.442	0.134	0.893
$[Mo_6Se_8(CN)_6]^{7-/8-}$	−0.876	0.083	0.933
$[Mo_6Se_8(CN)_6]^{8-/9-}$	−1.369	0.090	0.804
$[Mo_4Se_4(CN)_{12}]^{6-/7-}$	0.233	0.168	2.512
$[Mo_4Se_4(CN)_{12}]^{7-/8-}$	−0.422	0.058	0.224

depends on the condition of the electrode. One might expect one more redox process (at ∼ −1.8 V) for the $\mathbf{1}^{9-/10-}$ couple, since this would fill the e_g orbital to give a closed shell. However, the electrochemical potential window in these aqueous solutions does not allow us to scan to potentials more negative than −1.40 V without observing irreversible multielectron processes (probably water reduction).

Electrochemical data are presented for $\mathbf{1}^{n-}$ in Table 4. The peak potential separations (ΔE_p), 0.134(6−/7−), 0.083(7−/8−), and 0.090 V(8−/9−), are all larger than the nernstian value of 0.06 V. The peak current ratio (i_p^c/i_p^a) values range 0.892−0.933. The potential difference ($\Delta E_{1/2}$) between the 20/21, 21/22 CBE couples and 21/22, 22/23 CBE couples are 0.434 and 0.493 V, respectively. These increments ($\Delta E_{1/2} \sim 0.45$ V) between consecutive $E_{1/2}$ values are similar to values we have observed for other hexanuclear clusters in highly polar media when the redox processes involve the same or degenerate orbitals.[30,47−49]

These cyclic voltammetric data contrast sharply with measurements reported by Fedorov's group, who dissolved $K_7[\mathbf{1}^{7-}]\cdot 8H_2O$ in 0.1 M Na_2SO_4 (the working electrode was not reported).[27] Their reported cyclic voltammogram showed

(47) Sun, D.; Hughbanks, T. *Inorg. Chem.* **1999**, *38*, 992−997.
(48) Xie, X.; Hughbanks, T. *Angew. Chem., Int. Ed.* **1999**, *38*, 1777−1779.
(49) Xie, X.; Hughbanks, T. *Inorg. Chem.* **2000**, *39*, 555−561.

Table 5. Comparison of Reduction Potentials for $[Mo_4Se_4]^{n+}$ Species (Potentials vs SHE)

	$E_{1/2}$, V		
redox couple	$[Mo_4Se_4]^{6+/5+}$	$[Mo_4Se_4]^{5+/4+}$	ref
$[Mo_4Se_4(CN)_{12}]^{8-}$ in aq NaCN	0.233	−0.422	this work
$[Mo_4Se_4(CN)_{12}]^{6-}$ in aq Na_2SO_4	1.03	0.18	38
$[Mo_4Se_4(H_2O)_{12}]^{5+}$ in $HMeC_6H_4SO_3$	0.79	0.19	50
$[Mo_4Se_4(edta)_6]^{3-}$ in $LiClO_4$	0.65	−0.040	50

a one electron quasireversible oxidation wave at +0.63 V (vs SHE), and they stated that "further oxidation at 1.4 V is irreversible". Comparison with results from chemical reduction (below) clearly indicates that the potentials reported here correspond to redox processes for $[Mo_6Se_8(CN)_6]^{8-}$ species. It may be that the redox process measured by Fedorov's group is associated with a $[Mo_6Se_8]$ species, but under conditions in which hydrolysis of many, if not all, of the cyanide ligands had occurred.

A cyclic voltammogram recorded for a burgundy solution prepared by dissolving **5** in aqueous NaCN displayed two stepwise redox waves shown in Figure 5b. The potential was scanned over the range −0.68 to +0.67 V starting from −0.6 V and scanning in the negative initial direction. Two waves were observed with $E_{1/2} = 0.233$ and −0.422 V (vs SHE), respectively, corresponding to $\mathbf{2}^{6-/7-}$ and $\mathbf{2}^{7-/8-}$ couples. Since the t_2 HOMO is fully occupied for the $\mathbf{2}^{8-}$ ion and the HOMO−LUMO gap is large, further reduction of the intact cubane is effectively precluded: no additional waves were observed in a separate scan to negative potentials until we observe the onset of water reduction at ∼ −1.5 V.

Electrochemical data are presented for $\mathbf{2}^{n-}$ in Tables 4 and 5. The peak potential separations (ΔE_p) are 0.168(6−/7−) and0.058(7−/8−) for the couples. The 7−/8− couple has a potential separation smaller than 0.060 V, indicating that the electrode reaction is diffusion controlled. The peak current ratio (i_p^c/i_p^a) has values far from unity. Electrochemical measurements for other molybdenum cubane clusters ($[Mo_4Se_4(L)_{12}]^{n+}$, $n = 4, 5, 6$; L = CN^-, H_2O, edta) have been reported,[37,41,50,51] and those results are summarized in Table 5. The differences between our data and the results of Fedin et al. are notable since both purport to apply the same cyanide ligated clusters, $[Mo_4Se_4(CN)_{12}]^{n-}$. However, just as for the Mo_6Se_8-based clusters, we performed our measurements in basic solutions in the presence of excess cyanide, and the results of Fedin et al. were obtained in nominally neutral aqueous solutions using Na_2SO_4 as the electrolyte. The discrepancies between the two results suggests that these highly anionic clusters are extensively hydrolyzed under the latter conditions.

Chemical Reduction and Isolation of $Na_8[Mo_6Se_8(CN)_6]\cdot 20H_2O$ (4). Our cyclic voltammetric results indicated that appropriate reducing agents for preparing $\mathbf{1}^{8-}$ and $\mathbf{1}^{9-}$ should possess oxidation potentials greater than ∼0.88 and 1.37 V. Standard oxidation potentials for Zn in basic solution[52] suggested it would be thermodynamically sufficient for preparation of $\mathbf{1}^{8-}$:

$$Zn + 4X^- \rightleftharpoons ZnX_4^{2-} + 2e^-$$
$$E = +1.26\ (X^- = CN^-);\ +1.245\ (X^- = OH^-)$$

Zn reduction in KCN and KOH solutions does indeed occur, as evidenced by a color change from deep blue ($\mathbf{1}^{7-}$) to purple ($\mathbf{1}^{8-}$). Solutions thereby obtained exhibit rest potentials more negative than we measured for the $\mathbf{1}^{7-/8-}$ couple (∼ −0.9 V). Crystals obtained from these solutions reproducibly exhibited structures isotypic with the cubic "$K_7[Mo_6Se_8(CN)_6]\cdot 8H_2O$" reported by Fedorov.[27] Like the Fedorov group, we find that the cubic unit cell parameter (a) varies widely, from 15.463(5) to 16.099(2) Å under various conditions. For example, a different lattice parameter was observed when crystals were obtained by layering with methanol or by slowly evaporating the solvent, even when excess Zn was used to reduce the cluster in both instances. In some cases, the solutions were treated with excess KCN and in other cases with excess KOH; this also affected the lattice parameter. Variability in the lattice parameter is mirrored in irreproducible K^+ occupancies, and there is certainly the possibility that some of the "water molecules" were actually hydroxide ions. The use of NaCN circumvents most of these problems, and we were able to isolate a crystal in which the chemical formula was apparent and the refinement of the Na^+ sites presented little difficulty. When an excess of Zn with NaCN (1:4 ratio) is added to a $[Mo_6Se_8(CN)_6]^{7-}$ solution, its characteristic blue color quickly changes to a deep red, indicating the formation of $[Mo_6Se_8(CN)_6]^{8-}$:

$$2[Mo_6Se_8(CN)_6]^{7-}(aq) + Zn(s) + 4CN^-(aq) \rightleftharpoons$$
$$2[Mo_6Se_8(CN)_6]^{8-}(aq) + Zn(CN)_4^{2-}(aq)$$

The $[Mo_6Se_8(CN)_6]^{8-}$ solution is stable in the presence of excess reducing agent for several weeks. Zinc was removed by filtration, and addition of MeOH precipitated the red $Na_8Mo_6Se_8(CN)_6\cdot 20H_2O$ (**4**). When dry, **4** is very air sensitive, and some oxidation, regenerating the $\mathbf{1}^{7-}$ ion, is difficult to avoid.

The process of air oxidation of the $\mathbf{1}^{8-}$ ion can be monitored by use of UV−vis spectroscopy. As shown in Figure 6, oxidation of the $\mathbf{1}^{8-}$ ion is accompanied by a red shift in the absorption maximum at 540 nm by about 25 nm, and a barely discernible shoulder at ∼580 nm intensifies and shifts to about 595 nm. The observation of an isosbestic point (∼535 nm) indicates that the air-oxidation is a reasonably clean process, involving only $\mathbf{1}^{8-}$ and $\mathbf{1}^{7-}$. If a solution of $\mathbf{1}^{7-}$ is exposed to air for an extended period of time (several days), no shifting of peaks above 500 nm is observed, but absorption intensity steadily decreases as $\mathbf{1}^{6-}$ is formed. Since $\mathbf{1}^{6-}$ has

(50) Nasreldin, M.; Henkel, G.; Kampmann, G.; Krebs, B.; Lamprecht, G. J.; Routledge, C. A.; Sykes, A. G. *J. Chem. Soc., Dalton Trans.* **1993**, 737−746.
(51) McFarlane, W.; Nasreldin, M.; Saysell, D. M.; Jia, Z.-S.; Clegg, W.; Elsegood, M. R. J.; Murray, K. S.; Moubaraki, B.; Sykes, A. G. *J. Chem. Soc., Dalton Trans.* **1996**, 363−369.
(52) *Standard Potentials in Aqueous Solution*; Bard, A. J., Parsons, R., Jordan, J., Eds.; Marcel Dekker: New York, 1985.

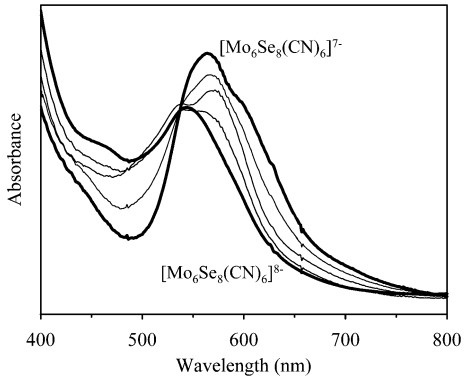

Figure 6. The UV−vis absorption spectrum of **4** (1 mM solution) illustrating the oxidation of $\mathbf{1}^{8-}$ to $\mathbf{1}^{7-}$.

no electrons in the e_g orbital, it is reasonable to assign the 580 and 540 nm (2.14 and 2.30 eV) absorptions for $\mathbf{1}^{8-}$ to $e_g \rightarrow t_{2u}$ transitions across the Mo−Mo bonding−antibonding gap. A DFT-BLYP calculation for the related chain compound **3** (using $k = 0$; no local point symmetry imposed) yields an estimated gap for the $e_g \rightarrow t_{2u}$ transition of 2.56 eV.

Conclusions

The chemistry surrounding cyanide salt synthesis of hexanuclear and tetranuclear molybdenum selenide clusters has been elucidated, and the stability of reduced cyano-ligated molybdenum selenide clusters in aqueous media has been demonstrated. The $[Mo_6Se_8(CN)_6]^{n-}$ and $[Mo_4Se_4(CN)_{12}]^{n-}$ clusters are quite stable in basic/cyanide-rich aqueous solutions. We have successfully synthesized the most reduced forms, $[Mo_6Se_8(CN)_6]^{8-}$ and $[Mo_4Se_4(CN)_{12}]^{8-}$. We have achieved a much improved understanding for the dissolution of the linear chain compound $K_6Mo_6Se_8(CN)_5$ (**3**), which is accomplished by redox catalysis of $[Mo_4Se_4(CN)_{12}]^{7-}$.

Acknowledgment. We wish to thank Lindsay Roy for calculations done on $Na_4Cs_7Mo_4Se_4(CN)_{12}Cl_3$ and $K_6Mo_6Se_8(CN)_5$ systems. We thank the Robert A. Welch Foundation for its support through Grant A-1132, the National Science Foundation for its support through Grant CHE-9623255, and the Texas Advanced Research Program through Grant 010366-0188-2001.

Supporting Information Available: X-ray crystallographic files in CIF format for the structure determinations. This material is available free of charge via the Internet at http://pubs.acs.org.

IC035050U